doi:10.1017/S1431927615010235 Paper No. 0944
Microsc. Microanal. 21 (Suppl 3), 2015

Analysis of Dislocation Densities using High Resolution Electron Backscatter Diffraction

Arantxa Vilalta-Clemente[1], Jun Jiang[2], Ben Britton[2], David M Collins[1] and Angus Wilkinson[1]

[1.] Department of Materials. University of Oxford, Parks Road, Oxford, OX1 3PH
[2.] Department of Materials, Imperial College London, Prince Consort Road, London, SW7 2AZ, UK

Cross-correlation analysis of electron backscatter diffraction (EBSD) patterns allows measurement of elastic strain and lattice rotation variations at a sensitivity of ~$\pm 10^{-4}$ [1]. Cross-correlation is used to measure shifts between sub-regions of test and reference patterns and simple geometry allows the elastic strains and lattice rotations to be calculated from the measured dispersion of pattern shifts. In deformed metals the lattice rotations are often significantly larger than the elastic strains and in these situations a pattern 'remapping' approach has proved necessary to avoid artefacts in the strain fields [2].

One area of application for EBSD has been the determination of dislocation densities. The most explored route for quantifying the dislocation density has been to use the relationship, described by Nye [3] between the geometrically necessary dislocation (GND) density and the lattice curvature. In Nye's analysis the excess density of dislocations in the crystal is directly related to the gradient of the lattice rotation field that induced. Unfortunately solution of the reverse problem of finding dislocation densities from the measured rotation gradients often does not have a unique solution. This situation is exacerbated by the fact that only 6 of the nine possible rotation gradient terms can be established from EBSD on a single section. Despite these issues, a lower bound estimate of the total dislocation density can be made (though the densities of particular dislocation types are ambiguous). Figure 1 shows an example map of GND density distribution within a Cu polycrystal deformed to 10% tensile strain. Of course the GND density is only a fraction of the total dislocation density because any dipoles or multipoles between the measurement points cause no measureable rotation gradient. This leads to differences in the GND density as the step size is varied. Figure 1 shows the GND density recovered in the same region but with the rotation gradients calculated using three different length scales. This is shown in a more quantitative way in figure 2 which shows how the average GND density recorded in this map reduces as the effective step size is made progressively larger [4].

To estimate the total dislocation density a new approach has been recently proposed [5]. This borrows from peak profile analysis used in X-ray and neutron diffraction assessment of dislocation density. From the EBSD data the variations of stress from the mean value in each grain can be calculated and used to form a plot showing the probability of obtaining a given stress level. In all dislocated crystal we have analyzed the probability has the form of a central Gaussian-like part but has tails showing higher probabilities at the high stress levels with the probability following $P(\sigma) = A/\sigma^3$. The form of these tails is consistent with the high stresses being generated by the localized stresses close to isolated dislocation cores, and the magnitude of the proportionality constant A can be used to determine the dislocation density. As the tails correspond to low probability, where experimental data tends to be somewhat noisy, rather than fitting the data directly we follow Groma's method [5] developed for analysis of X-ray diffraction peak intensities of using the restricted second moment V_2 of the probability

$$V_2(\sigma) = \int_{-\sigma}^{+\sigma} P(\sigma)\, \sigma^2 \, \mathrm{d}\sigma$$

For the large shear stress σ_{xy} close to an isolated edge dislocations with Burgers vector magnitude b along the x-axis and line direction along the z-axis normal to the sample surface of an isotropic elastic medium of shear modulus G and Poisson ratio, ν, it can be shown that

$$V_2(\sigma) = \frac{(G\,b)^2}{8\pi(1-\nu)^2}\rho_0 \ln(\sigma/\sigma')$$

Thus at large stresses we expect a plot of V_2 against $\ln(\sigma)$ to tend toward a straight line, and the gradient of this is related to the total dislocation density ρ_0 [6]. Figure 3 shows some examples of such plots for a ferritic steel in the annealed condition and after cold rolling to various reductions, and the total dislocation density obtained from the gradients is shown in the figure.

Further evidence that the high stress values obtained at local positions by EBSD mapping is due to the incident beam being very close to dislocation positions is found by comparing the electron channeling contrast imaging (ECCI) and EBSD results. Figure 4 makes this comparison for a GaN sample which contains threading dislocations revealed as black/white dots in ECCI (figure 4a). The corresponding EBSD generated elastic strain fields show local 'spikes' in the vicinity of the dislocations (ε_{xy} map in figure 4b).

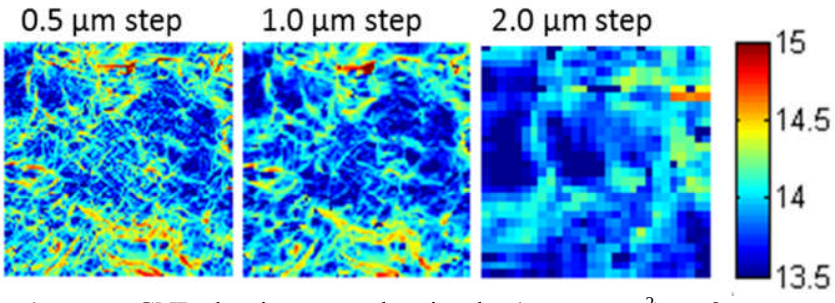

Figure 1: GND density maps showing log(ρ_{GND} in m^{-2}) in the same region of a Cu sample deformed to 2% mapped at different effective step sizes.

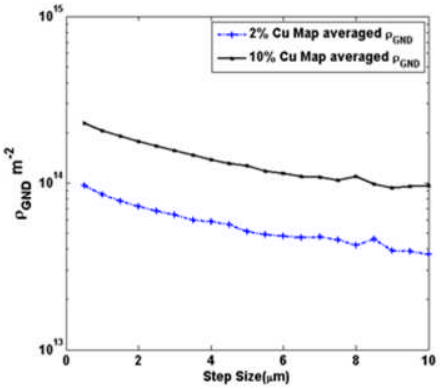

Figure 2: GND density variation with step size for Cu samples deformed to 2% and 10%.

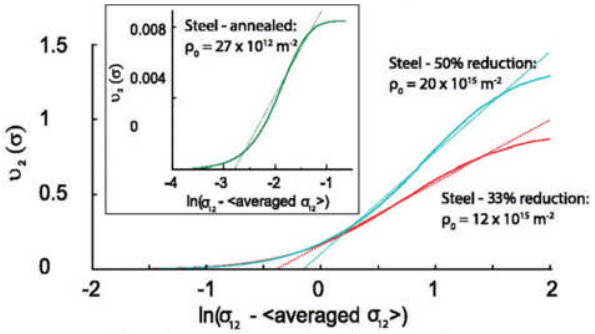

Figure 3: Plots of restricted second moment of stress probability distribution against ln(stress) from which the total dislocation density can be determined. Data for ferritic steel before and after cold rolling.

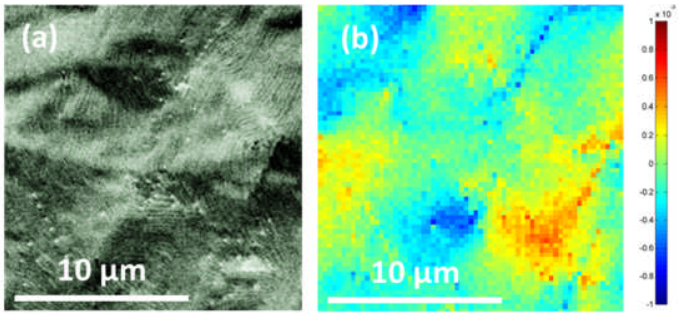

Figure 4: (a) ECCI and (b) EBSD maps showing localized elastic strain (ε_{xy}) 'spikes' near threading dislocations in GaN.

References:
[1] A.J. Wilkinson, G. Meaden, and D.J. Dingley, Ultramicroscopy **106** (2006), p. 307.
[2] T.B. Britton and A.J. Wilkinson, Ultramicroscopy **114** (2012), p. 82.
[3] J.F. Nye, Acta Metallurgica **1** (1953), p. 153.
[4] J. Jiang, T.B. Britton and A.J. Wilkinson, Ultramicroscopy, **125** (2013), p. 1.
[5] I. Groma, Physical Review B **57** (1998), p. 7535.
[6] A.J. Wilkinson *et al*, Applied Physics Letters **105** (2014), p. 181907.
[7] We acknowledge ESPRC funding under grants EP/K034332/1, EP/J016098/1, & EP/I021043/2.